Observation of Spherical Focus in an Electron Penning Trap

T. B. Mitchell* and M. M. Schauer
Physics Division, Los Alamos National Laboratory, Los Alamos, New Mexico 87545

D. C. Barnes
Theoretical Division, Los Alamos National Laboratory, Los Alamos, New Mexico 87545
(Received 11 September 1996)

We produce simultaneously dense and well-confined nonneutral plasmas by spherical focusing. A small (3 mm radius) Penning trap has low-energy electrons injected at a single pole of the sphere. Precisely when the trap parameters are adjusted to produce a spherical well, the system self-organizes into a spherical state through a bootstrapping mechanism which produces a hysteresis. Additional confirmation of the dense spherical focus is provided by electrons scattered by the central core. Core densities up to 35 times the Brillouin density have been inferred from the data. [S0031-9007(96)02081-9]

PACS numbers: 52.25.Wz, 52.25.Fi

In contrast to quasineutral, magnetic confinement laboratory plasma devices, Penning traps [1] have exhibited remarkable confinement of nonneutral plasmas. However, due to the charge nonneutrality of these plasmas, the uniform densities attainable in static traps are limited, the maximum value being the Brillouin limit $\overline{n} \equiv B^2/2\mu_o mc^2$ (where B is the magnetic field, μ_o the permeability of free space, m the mass of confined particles, and c the speed of light) [2]. Here we describe experimental results from the Penning fusion experiment (PFX), an investigation into the possibility of raising confined densities (through spatial nonuniformity) to levels of interest for thermonuclear fusion applications while retaining the excellent confinement of thermal nonneutral plasmas [3].

In its simplest form a Penning trap consists of three electrodes, the inner surfaces of which are hyperbolae of revolution [4]. Two end cathode caps and a central anode ring (see Fig. 1) produce a rotationally symmetric electrostatic quadrupole field when a voltage V is applied to the anode. Charged particles are confined axially in the electrostatic well, while radial confinement is provided by a uniform magnetic field applied parallel to the trap axis. As previously noted [3] the eccentricity of the resulting spheroidal well is tunable. As V is increased at constant B, the limiting equipotential of the trap changes from a prolate spheroid intersecting the end cathodes and preventing electrons from reaching the anode, to a sphere nearly intersecting both the cathodes and anode, to an oblate spheroid which intersects the end cathodes and a portion of the anode.

A low-energy, zero canonical angular momentum electron in a spherical well will oscillate along the trap axis through the center of the well. Any scattering event which occurs at or near the center of the trap will deflect the electron away from the trap axis onto an orbit which will necessarily pass near the trap center again. In the absence of collective effects, a collection of such electrons will result in a nonneutral plasma with an enhanced central density due to the spherical convergence of the single particle orbits. In this Letter we report the observation of such a density focus.

The PFX trap electrodes are fashioned from titanium due to its superior vacuum and high voltage characteristics. The inner diameter of the anode ring is 6 mm, as is the minimum separation of the two end cathode caps. Both of the end cathodes are pierced through the center by 400 μm diameter holes which allow injection of electrons into the trap via the lower end cathode, while providing diagnostic access through the upper one.

Low angular momentum electrons are provided by a LaB_6 crystal emitter situated a short distance behind the hole in the lower end cathode (Fig. 1). The emitter consists of a cone with a 60° included angle ending in a 200 μm diameter flat surface. Most of the emission originates on this flat surface, thereby producing a uniform, 200 μm diameter beam.

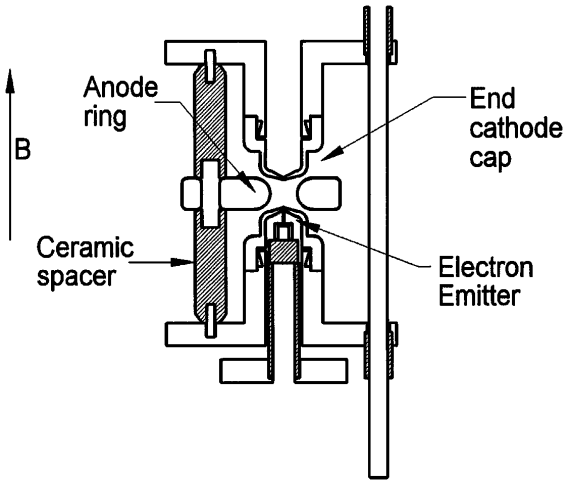

FIG. 1. PFX hyperbolic trap. The three electrodes are suspended by three support rods and mechanically connected by ceramic spacers whose cathode ends are tailored to maximize voltage standoff. An emitter is placed near the injection hole in the lower cathode.

 0031-9007/96/78(1)/58(4)$10.00

The trap assembly is contained within a stainless steel vacuum vessel that is inserted into the bore of a superconducting magnet. As the magnet is operated in cold bore configuration, the trap is held at liquid helium temperature. Typical operating voltages range from 500 V to 10 kV, with the corresponding magnetic fields necessary to produce a spherical well ranging from 0.05 to 0.22 T.

Above the trap, in the fringe of the magnetic field, sits a microchannel plate/phosphor screen (MCP) assembly. Electrons can be transported from the trap, through the hole in the upper end cathode and two independently biasable drift tubes, to the MCP. The MCP can be used in a particle counting mode by means of a multichannel scaler, or in an imaging mode by capturing phosphor screen images with a CCD camera and frame grabber.

Typical operation is as follows. First, the magnetic field is set to the desired value and the voltages applied to the upper and lower end cathodes are set to their nominal values, usually within a few tens of volts of ground. Next, the anode voltage is ramped to the desired value and electron current into the trap I_i is started. Usually the electron beam is reflected back upon itself by biasing the upper end cathode more negatively with respect to ground than the emitter crystal.

Measurements of currents to various electrodes can then be made. Total current scattered from the beam to the anode I_A may be measured, and electrons scattered up in energy, and thus able to climb over the barrier presented by the upper end cathode, may be counted at the MCP. After some predetermined time, I_i is turned off and V is ramped to zero. As V is decreased, some of the electrons which have lost energy, and thus become trapped, escape the well and are counted at the MCP. One is now ready to repeat the measurements or move to a new magnetic field value.

A remarkable feature of the observations is the spontaneous appearance of a nearly spherically symmetric state. This occurs only when B and V are adjusted to produce a spherical well according to

$$V_o = \frac{eB^2a^2}{8m_e}, \tag{1}$$

where e and m_e are the electron charge and mass, and a the trap radius [5]. Then if I_i exceeds a threshold current, a spherical state appears. Several indicators of this are shown in Fig. 2.

In Fig. 2(a) the current collected on the anode, I_A, is shown as a function of anode voltage, V, at fixed B. At the lowest I_i shown, essentially none of the injected current reaches the anode, while at higher I_i up to $\sim 15\%$ is collected there. This result is interpreted as follows. When the well is spherical, electrons passing near the trap center are reflected back nearly to the center. A spherical density focus will be formed if I_i is high enough to provide sufficient central space charge to deflect a portion of the injected beam away from prompt loss back through the injection hole. Electrons so deflected will reflex a number of times back near the center, contributing to the growing space charge of the central core. This bootstrapping mechanism will continue until a steady-state equilibrium, with electrons ergodically filling the spherical well and producing a dense central core, is reached [5].

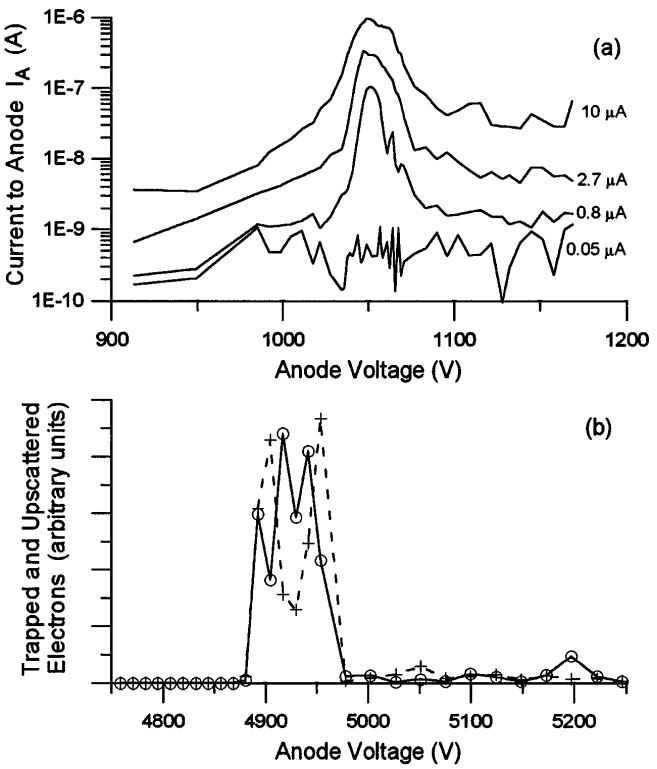

FIG. 2. These data are a coincident indication of an elastic scattering process occurring only near the spherical point. (a) Observed anode current vs anode voltage V near the spherical point for $B = 0.076$ T. As the injection current (indicated) is increased a sharp resonance appears at $V = V_o$ and broadens slightly. (b) Observed upscattered (solid curve) and trapped/downscattered electrons (dashed curve) vs V near a second spherical point ($B = 0.164$ T). The double maxima of the dashed curve is an artifact caused by amplifier saturation.

Such a mechanism should be operative only when the trap parameters are nearly spherical. This is consistent with the observations that maximum I_A is observed near (essentially at) the "spherical point" where $V = V_o$, and that at values of V above the spherical point I_A is observed to decrease strongly, even though injected electrons are energetically able to reach the anode.

Other diagnostics further support the interpretation. Figure 2(b) shows, for a similar V scan, the detection of electrons upscattered and downscattered in energy. These electrons are interpreted to have been scattered by elastic interactions with the dense core. The same resonance width is indicated by all three diagnostics of Fig. 2; this resonance width increases with I_i from around 1% to a few percent of V_o.

Figure 3 shows additional effects of trapped charge. Two sequences of I_A vs I_i are shown at a fixed spherical point ($B = 0.072$ T, $V = 940$ V). The discrete points are the results of cyclic measurements, in which I_A is

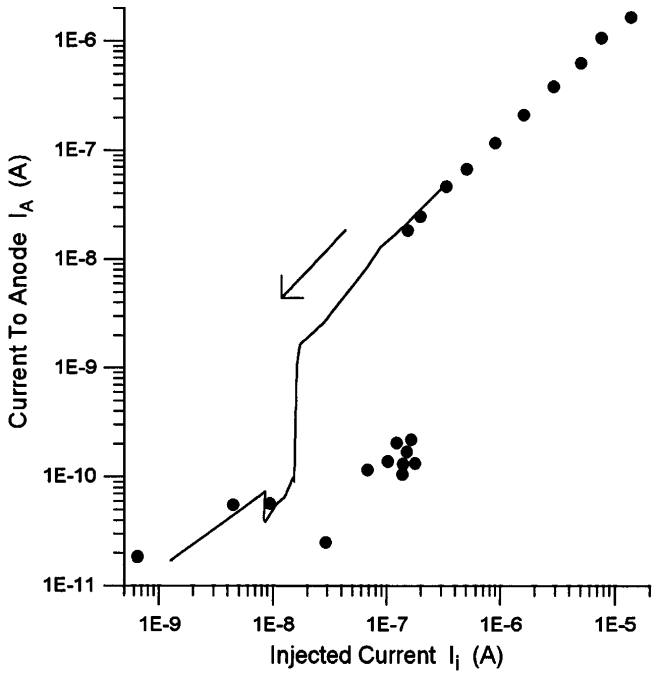

FIG. 3. Hysteresis curve for the spherical state at fixed spherical point, $B = 0.072$ T, $V = 940$ V. Solid circles are individual filling cycles, while continuous curve is quasistatic decrease of I_i. As I_i is increased (abscissa), I_A (ordinate) suddenly rises, indicating a transition from a beamlike state to a spherical state. The hysteresis observed as I_i is continuously decreased is consistent with trapped injected beam electrons serving as a "seed" core allowing the continuation of the spherical state.

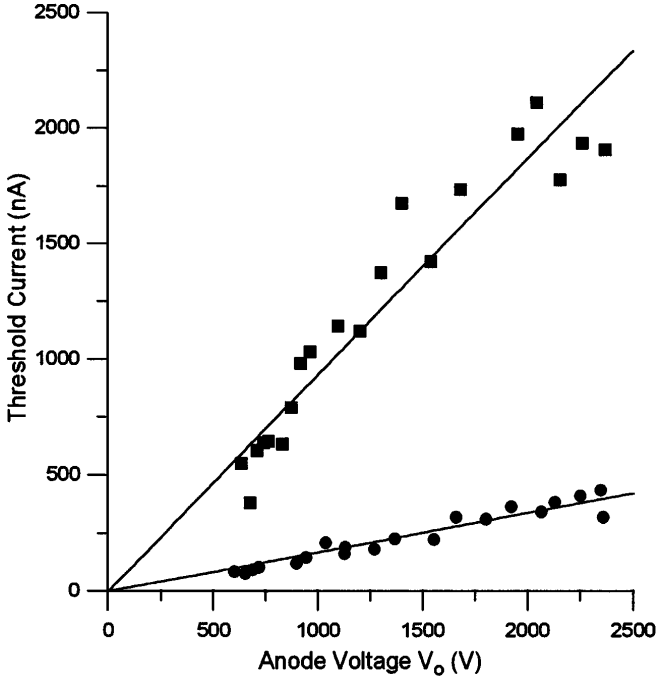

FIG. 4. Threshold I_i as a function of anode voltage V_o for a series of spherical points. Upper curve (squares) is with injected beam passing through upper cathode, while lower beam (circles) is with injected beam reflected from upper cathode. The lines are linear fits through the origin.

recorded, and the trap is emptied before I_i is increased and a new measurement of I_A is made. At a threshold value ($I_i \approx 150$ nA), I_A increases dramatically. The continuous line represents a sequence of data, obtained at the same spherical point but with continuous operation, during which I_i is decreased on a time scale of several seconds. That is, the trap is not emptied between each measurement of I_A. At a much lower threshold ($I_i \approx 15$ nA) I_A returns to its low value.

The presence of the threshold is consistent with the electron beam producing a trapped population within the well, which at a certain I_i becomes large enough to deflect a significant portion of the beam. Hysteresis in the anode current as I_i is decreased below the threshold is a result of the presence of this trapped population which acts as a seed for the focus.

The scaling of threshold I_i with V, where B has been set to the spherical point, is shown in Fig. 4. Two sequences, corresponding to different operation of the upper end cathode, both indicate linear variation of the threshold. In the case of higher threshold, the upper cathode potential is such that the injected beam passes directly through the trap, while in the lower case the beam is reflected back toward the injector. The quantitative difference of the two sequences represents recirculation of the reflected beam for a few transits.

It can be shown [5] that the deflected fraction of the incoming beam is proportional to the ratio of the trapped inventory to the Brillouin inventory $\overline{N}$. The Brillouin inventory is defined as that which fills the trap sphere with a uniform plasma of density $\overline{n}$. Since both $\overline{N}$ and V_o are proportional to B^2, it follows that $\overline{N}$ varies linearly with V_o. As the trap inventory is proportional to I_i, one expects the threshold current to scale linearly with V_o, as is seen to be the case.

Spherical focusing has been observed over the range of PFX operation. Figure 5 shows a summary of the observation of three diagnostics over the range of B and V, compared to the theoretical relation of Eq. (1). As can be seen the agreement is excellent, with focusing indicated only for points within 1% of the curve given by Eq. (1).

A few additional observations are mentioned in passing as an indicator for future work. First, there are significant effects from increasing I_i. These include a broadening of the resonance as shown in Fig. 2(a), and wave activity observed as induced fluctuations of the electrode voltages. These phenomena may be associated with large space charge effects on the formation and maintenance of the spherical focus. For example, it may be that at values of I_i far above the threshold value for spherical formation there is some shielding of the applied well toward a spherical one, with associated resonance broadening and sensitivity of the focus to collective effects.

An additional observation is that the focus shown by the data here is degraded if the intrinsic field error of the device

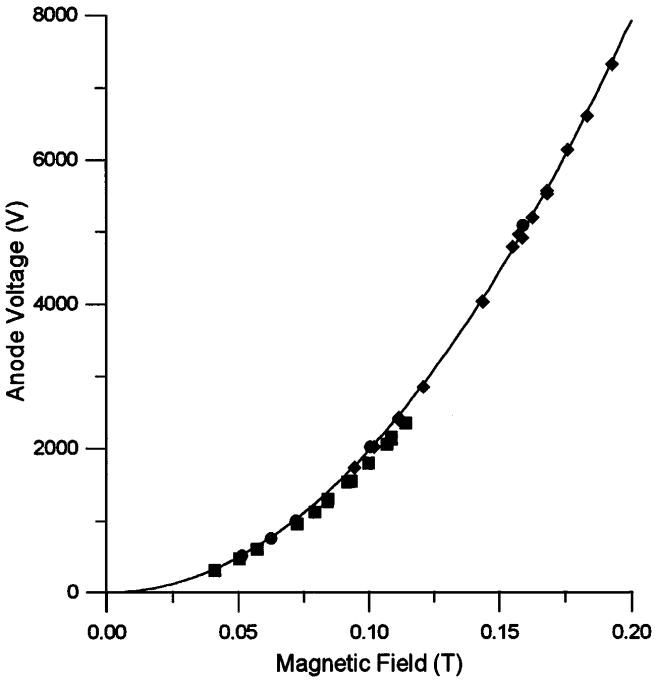

FIG. 5. Summary of three data indicative of spherical state. Locations of maximum I_A (squares), upscattered electrons (diamonds), and downscattered electrons (circles) are shown vs anode voltage V and magnetic field B. The curve is the calculated theoretical spherical condition of Eq. (1).

is made too large. In one series of experiments the axial separation of the cathodes from the anode was decreased by 250 μm, introducing an error in the electrostatic field of about 5%. Under this condition no appreciable focusing was observed in any of the diagnostics. This seems to indicate that the intrinsic field error is of order 1% or less in PFX. The focus is also degraded if the injected beam is too asymmetric; during one experimental series, the emitter developed a lobed emission pattern and the focus was not obtained.

The present results, combined with a theoretical analysis, indicate that PFX has achieved the desired spherical focus over a range of well depths. The indicators of this are: a sharp resonance whose width ($\sim$1%) is expected to be comparable to the ratio of the core radius to the trap radius [5]; the sudden transition to large angle deflections of injected electrons, indicating the appearance of significant central space charge; expected scaling with B, V, and I_i; and sensitivity of the focus (resonance) to field and injection errors.

A numerical model has been developed and applied to compute the electron distribution produced in PFX [5]. In this model the electron distribution is assumed to depend only on the spherical radius and velocity and to evolve according to classical, small-angle collisions according to the fully nonlinear Fokker-Planck model. The radial effective potential includes the applied spherical well and the space charge of the confined electrons. Using sources and losses consistent with PFX parameters, it is found that a focused state is formed and maintained with a density core of radius 30 μm and a density of $35\overline{n}$. The consistency of the observations with this computed state suggests that the electron behavior in PFX is classical and that the Brillouin density has indeed been significantly exceeded by formation of a spherical focus.

Future work with the PFX device will utilize a gas puff diagnostic to produce a quasineutral, D-T thermonuclear core plasma. For the purposes of generation of fusion power, however, the current device can be shown [3] to be limited by high voltage breakdowns to modest thermonuclear gain ($Q \sim 10^{-4}$). For higher Q, a modified geometry, such as replacement of the low-order multipole fields of the spherical Penning trap with a high-order multipole system, will be necessary.

This work was sponsored by the Office of Fusion Energy Science of the U.S. Department of Energy.

*Present address: MS 847.11, National Institute of Standards and Technology, Boulder, Colorado 80303.

[1] *Non-neutral Plasma Physics,* edited by C. W. Roberson and C. F. Driscoll (American Institute of Physics, New York, 1988); *Non-neutral Plasma Physics II,* edited by J. Fajans and D. H. E. Dubin (American Institute of Physics, New York, 1995); R. C. Davidson, *Physics of Nonneutral Plasmas* (Addison-Wesley, Redwood City, California, 1990).

[2] L. Brillouin, Phys. Rev. **67**, 260 (1945).

[3] D. C. Barnes, R. A. Nebel, L. Turner, and T. N. Tiouririne, Plasma Phys. Controlled Fusion **35**, 929 (1993).

[4] L. S. Brown and G. Gabrielse, Rev. Mod. Phys. **58**, 233 (1986).

[5] D. C. Barnes, T. B. Mitchell, and M. M. Schauer (to be published).